

# Probing the formation process of aluminium hydroxide nanoparticles prepared by laser ablation with $^{27}\text{Al}$ NMR spectroscopy

Hsien-Ming Kao,<sup>\*a</sup> Ru-Rong Wu,<sup>b</sup> Tung-Yu Chen,<sup>b</sup> Yu-Hung Chen<sup>b</sup> and Chen-Sheng Yeh<sup>\*b</sup>

<sup>a</sup>Department of Chemistry, National Central University, Chung-Li, Taiwan, 32054.

E-mail: hmkao@cc.ncu.edu.tw

<sup>b</sup>Department of Chemistry, National Cheng Kung University, Tainan, Taiwan, 701.

E-mail: csyeh@mail.ncku.edu.tw

Received 20th June 2000, Accepted 6th September 2000

First published as an Advance Article on the web 18th October 2000

The  $^{27}\text{Al}$  MAS NMR spectra of amorphous alumina exhibit three resonances resulting from aluminium in four-, five-, and six-coordination, whereas samples containing crystalline particles of bayerite, gibbsite, and boehmite show only a single resonance associated with six-coordinate aluminium.

## Introduction

Nanoscale materials have attracted considerable attention because of their potential applications in catalysis, bioanalysis, and electronic devices.<sup>1,2</sup> For example, metal oxides and hydroxide colloids containing aluminium are important in the ceramics industry.<sup>3</sup> Recently, we have prepared aluminium hydroxides, *i.e.*,  $\text{Al}(\text{OH})_3$  and  $\text{AlOOH}$ , in  $\text{H}_2\text{O}$  by the laser ablation method.<sup>4</sup> Immediately after preparation, the nascent gels exhibited an amorphous structure with a broad reflection between  $10^\circ$  and  $50^\circ$  in their XRD patterns. Some spherical particles with high-density contrast, which were identified as boehmite, appeared in the resulting gels as well. Through the course of aging, bayerite, gibbsite and boehmite particles were formed simultaneously. A dissolution–recrystallization process was observed in the development of these aluminous materials. Unfortunately, such transformation mechanisms involving structure changes remain ambiguous.

Solid state NMR is an atomic scale, element-specific probe that is able to identify local coordination environments, usually *via* the isotropic chemical shift.  $^{27}\text{Al}$  magic angle spinning (MAS) NMR has been widely used to probe the local order in different types of aluminium-containing materials and its evolution during the synthesis process, since  $^{27}\text{Al}$  chemical shifts can be correlated with the coordination number of aluminium in Al–O compounds. An important feature of  $^{27}\text{Al}$  solid state NMR is the dependence of the isotropic chemical shift ( $\delta_{\text{iso}}$ ) of the central ( $+1/2$ ,  $-1/2$ ) resonance on local Al coordination:  $\text{AlO}_4$  (*ca.* 80 to 45 ppm) and  $\text{AlO}_6$  (*ca.* 20 to  $-20$  ppm). Usually, peaks in the range *ca.* 45 to 20 ppm are taken to result from  $\text{AlO}_5$  polyhedra.<sup>5</sup> Moreover, depending on the local symmetry, the  $^{27}\text{Al}$  resonances suffer from broadening due to quadrupolar interactions which can be large enough that second-order effects become important. This can hamper an unambiguous assignment and analysis of the spectra.

In this work,  $^{27}\text{Al}$  MAS NMR was employed to characterize the Al coordination and the development of order in the formation of aluminous nanoscale particles.

## Experimental

### Preparation of alumina nanoparticles

The preparation of aluminous materials for these experiments has been described previously.<sup>4</sup> Briefly, a rotating Al rod (99.9999%), immersed in 5 ml of triply distilled water, was

irradiated using a wavelength of 532 nm of the second harmonic output of an Nd:YAG laser (Quantel Brilliant). During the process of aging, samples were stored in Pyrex bottles with caps, sealed under aerobic conditions. Samples were collected and then dried in a vacuum desiccator for NMR measurements. TEM images were obtained on a Zeiss 10C (80 kV) instrument.

### $^{27}\text{Al}$ MAS NMR measurements

$^{27}\text{Al}$  MAS NMR experiments were carried out at room temperature on a Bruker AVANCE-400 spectrometer operating at 104.3 MHz. A 4 mm doubly bearing MAS probe was used with a spinning speed of 12 kHz.  $^{27}\text{Al}$  Bloch decay spectra were recorded with a short excitation pulse, usually 0.6  $\mu\text{s}$  (equivalent to  $10^\circ$  pulse length), and a recycle delay of 1 s to ensure a quantitative interpretation of the data.<sup>6</sup> Chemical shifts are referenced with respect to an external  $\text{Al}(\text{NO}_3)_3$  aqueous solution.  $^1\text{H} \rightarrow ^{27}\text{Al}$  cross-polarization (CP) MAS spectra were recorded with contact times varying from 50  $\mu\text{s}$  to 10 ms, a  $^1\text{H}$   $\pi/2$  pulse of 4 ms, a recycle decay of 2 s and a spinning speed of 12 kHz. Since only the central transition is observed, excitation in the  $^1\text{H} \rightarrow ^{27}\text{Al}$  CP MAS experiments is selective and, therefore, the Hartmann–Hahn condition can be met when  $3\gamma_{\text{Al}}B_{\text{Al}} = \gamma_{\text{H}}B_{\text{H}} \pm n\omega_{\text{r}}$ , where  $\gamma_{\text{Al}}$  and  $\gamma_{\text{H}}$  are the gyromagnetic ratios of aluminium and proton spins, respectively,  $B_{\text{Al}}$  and  $B_{\text{H}}$  are the radio frequency field strengths applied on both nuclei,  $\omega_{\text{r}}$  is the spinning speed, and  $n$  is an integer.<sup>7,8</sup> The Hartmann–Hahn condition was established on a sample of kaolinite.

## Results and discussion

### $^{27}\text{Al}$ MAS NMR

$^{27}\text{Al}$  NMR results provide atomic scale information that can be combined with the complementary information from TEM to build a comprehensive picture of the phases present and their structures. Fig. 1(a) shows the inhomogeneous spherical aluminous material in a state of agglomeration in the nascent solutions. The corresponding  $^{27}\text{Al}$  Bloch decay and  $^1\text{H} \rightarrow ^{27}\text{Al}$  CP NMR spectra can be seen in Fig. 1(b), where the resonances at 67 ppm have been plotted with normalized intensities. Both spectra display three broad resonances. The resonances at approximately 7 and 67 ppm can be straightforwardly assigned to six- and four-coordinate aluminium, respectively. The

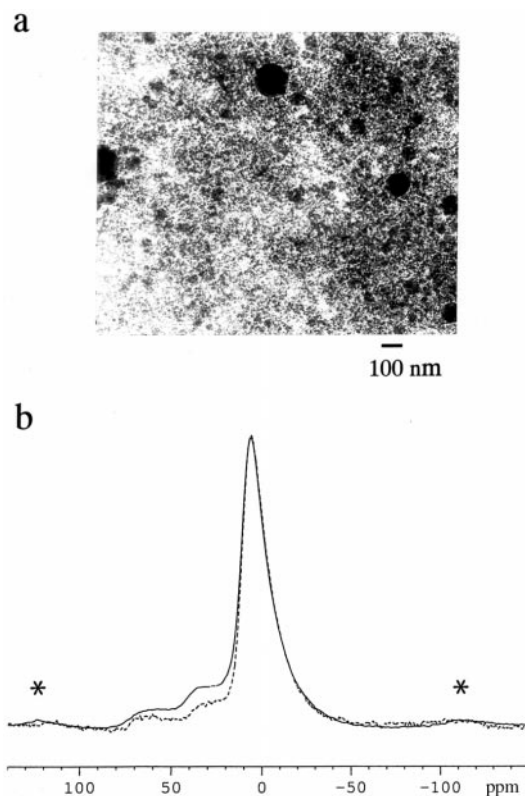


**Fig. 1** (a) TEM image obtained for a nascent solution under irradiation at 532 nm using 80 mJ per pulse for a 30 min exposure time. (b)  $^{27}\text{Al}$  Bloch decay (solid line) and  $^1\text{H}\rightarrow^{27}\text{Al}$  CP MAS (dashed line) NMR spectra of the amorphous sample. Asterisks denote spinning sidebands.

resonance at approximately 35 ppm is attributable to five coordinate aluminium, since the same resonance has also been observed in a number of aluminium-containing compounds.<sup>9,10</sup> It could correspond to unsaturated aluminium ion in an octahedral position (pentacoordinated aluminium ion), as observed in sol-gel alumina samples.<sup>11</sup> The resonance at around 67 ppm with low signal intensity can be ascribed to tetrahedrally coordinated aluminium centers in Keggin-type cations, *i.e.*, the  $[\text{Al}_{13}\text{O}_4(\text{OH})_{24}(\text{H}_2\text{O})_{12}]^{7+}$  polycation.<sup>12</sup> Assih *et al.* postulated the presence of boehmite particles in alumina sols, which are stabilized by  $\text{Al}_{13}$  polycations existing at the surface of these particles.<sup>12</sup> Furthermore, the resonance for boehmite gel has been determined to be near 7 ppm,<sup>13</sup> which is in good agreement with the observed chemical shift of the peak due to the six-coordinate aluminium studied here.

To gain more insight into the quantitative ratios of four-, five-, and six-coordinate aluminium, the Bloch decay spectrum of the amorphous sample was deconvoluted assuming that the lineshapes can be fitted by Gaussians. Since the electric field gradient (EFG) is different at each of the three sites and a distribution of EFGs exists, the peaks have different and asymmetrical lineshapes. These effects were taken into account by allowing the peaks for each site to be a linear combination of one, two or three Gaussians with different widths and positions. Good fits were obtained with relative intensities of approximately 1:1.3:13 for the 4-, 5-, and 6-coordinated aluminium, respectively, from the aluminous materials in Fig. 1(a).

#### $^1\text{H}\rightarrow^{27}\text{Al}$ cross-polarization

The  $^1\text{H}\rightarrow^{27}\text{Al}$  CP MAS spectrum [Fig. 1(b), dashed line] reveals the slight decrease in the intensities of both four- and five-coordinate Al species. Since only aluminium, which is coupled to the hydroxyl groups, will give signals in the  $^1\text{H}\rightarrow^{27}\text{Al}$  CP MAS experiment, the appearance of three

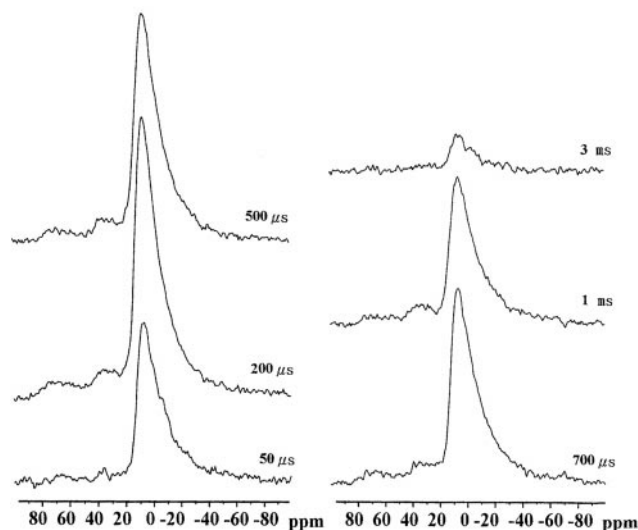


**Fig. 2** Variable contact time  $^1\text{H}\rightarrow^{27}\text{Al}$  CP MAS spectra of the amorphous sample. Spectra are plotted with their absolute intensities and different contact times are labeled.

resonances indicates the presence of three different kinds of Al sites which are connected with either hydroxyl groups or accessible to water molecules. The poorer CP efficiency of the four- and five-coordinate Al species suggests that these aluminium spins might be more distant from proton spins compared to the six-coordinate aluminium. Fig. 2 shows a series of  $^1\text{H}\rightarrow^{27}\text{Al}$  CP MAS NMR spectra with contact times of 50  $\mu\text{s}$  to 3 ms. The maximum signal intensity for all three resonances is obtained at a contact time of 200  $\mu\text{s}$ . The signal at 67 ppm reaches approximately 50% of its maximum intensity within a contact time of 50  $\mu\text{s}$ . Such efficient polarization transfer at such short contact times cannot be attributed to the protons of physisorbed water, since dehydration of the as-prepared material at 473 K under vacuum does not appreciably alter the CP intensity for comparable experimental parameters. Thus, the cross-polarization behavior at short contact times (50–700  $\mu\text{s}$ ) is most likely due to Al–OH groups, supporting the presence of octahedral Al atoms connected by shared OH groups.

Fig. 3 shows the TEM image and the  $^{27}\text{Al}$  Bloch decay NMR spectrum for the crystalline sample containing bayerite, gibbsite and boehmite particles, which result in only one single peak at approximately 8 ppm corresponding to six-coordinate aluminium, with a chemical shift consistent with that reported for crystalline boehmite in the literature.<sup>14</sup> It is known that both the local structures of bayerite and boehmite are oxygen octahedra, but two-thirds of the octahedral interstices are occupied by aluminium in gibbsite.<sup>15–17</sup> The course of aging, involving the dissolution–recrystallization process, has the effect on transforming the low-coordination aluminium sites into the more symmetrical and stable high-coordination sites. A change in the coordination of tetrahedral species has also been observed during sol preparation and aging, leading to the formation of (pseudo) crystalline boehmite, depending on the pH, temperature, and time of aging.<sup>18</sup> The full width at half height of the six-coordinate Al resonance for the crystalline sample becomes narrower compared to that for the amorphous sample, decreasing from approximately 1.8 kHz for the latter to 1.2 kHz for the former. A symmetric lineshape is also observed for the crystalline sample, indicating the well-ordered  $^{27}\text{Al}$  local environment. This is in good agreement with the observed changes in the TEM images. The observation indicates that the octahedrally coordinated aluminium center is an essential part of the resulting alumina sample. For a more precise characteriza-

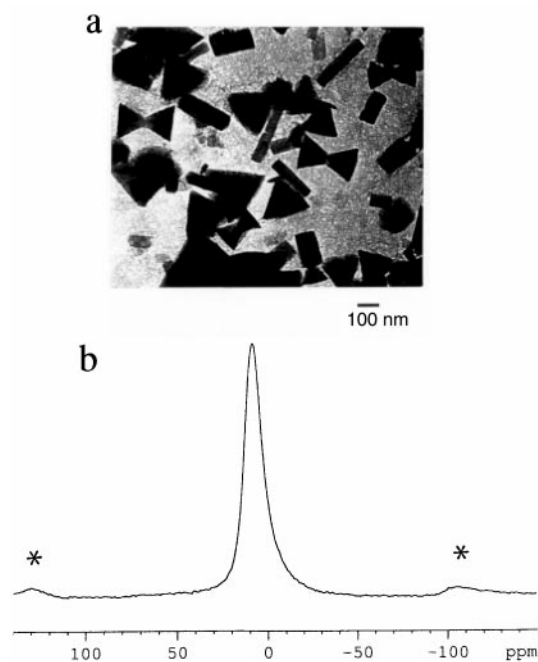


**Fig. 3** (a) Formation of bayerite (triangular), gibbsite (rectangular) and boehmite (background material) after aging for 3 days. Preparation conditions, *i.e.*, laser fluence and irradiation time, are the same as those in Fig. 1. (b)  $^{27}\text{Al}$  Bloch decay NMR spectrum of the crystalline sample. Asterisks denote spinning sidebands.

tion of the intermediate alumina species, further investigations would be required.

### Conclusions

$^{27}\text{Al}$  Bloch decay and  $^1\text{H} \rightarrow ^{27}\text{Al}$  CP MAS NMR spectroscopy have been used to probe the changes in local structure and aluminium coordination of aluminium hydroxides prepared *via*

the laser ablation method. The  $^{27}\text{Al}$  NMR spectra are also consistent with the observations from TEM images.

### Acknowledgements

Support from the National Science Council of the Republic of China is gratefully acknowledged.

### References

- 1 E. Braun, Y. Eichen, U. Sivan and G. Ben-Yoseph, *Nature*, 1998, **391**, 775.
- 2 C. R. Martin and D. T. Mitchell, *Anal. Chem.*, 1998, **70**, 322A.
- 3 F. F. Lange, *J. Am. Ceram. Soc.*, 1989, **72**, 3.
- 4 Y. P. Lee, Y. H. Liu and C. S. Yeh, *Phys. Chem. Chem. Phys.*, 1999, **1**, 4681.
- 5 M. E. Smith, *Appl. Magn. Reson.*, 1993, **4**, 1.
- 6 D. Freude and J. Haase, *NMR Basic Principle and Progress*, Springer-Verlag, Berlin, 1993.
- 7 W. Kolodziejski and A. Corma, *Solid State Nucl. Magn. Reson.*, 1994, **3**, 177.
- 8 A. Vega, *J. Solid State Nucl. Reson.*, 1992, **1**, 17.
- 9 L. B. Alemany and G. W. Kirker, *J. Am. Chem. Soc.*, 1986, **108**, 6158.
- 10 M. C. Cruickshank, L. S. Dent Glasser, S. A. Barri and J. F. Poplett, *J. Chem. Soc., Chem. Commun.*, 1986, 23.
- 11 J. A. Wang, X. Bokhimi, A. Morales and O. Novaro, *J. Phys. Chem. B*, 1999, **103**, 299.
- 12 T. Assih, A. Ayril, M. Abenoza and J. Phalippou, *J. Mater. Sci.*, 1988, **23**, 3326.
- 13 S. Komarneni, R. Roy, C. A. Fyfe and G. J. Kennedy, *J. Am. Ceram. Soc.*, 1985, **68**, C-243.
- 14 E. Morgado, Y. Lau Lam, S. M. C. Menezes and L. F. Nazar, *J. Colloid Interface Sci.*, 1995, **176**, 432.
- 15 B. R. Baker and R. M. Pearson, *J. Catal.*, 1974, **33**, 265.
- 16 R. F. Giese, *Acta Crystallogr. Sect. B*, 1976, **32**, 1719.
- 17 C. Sweegers, W. J. P van Enkevort, H. Meekes, P. Bennema, I. D. K. Hiralal and A. Rijkeboer, *J. Crystal Growth*, 1999, **197**, 244.
- 18 K. Sinko, R. Mezei, J. Rohonczy and P. Fratzl, *Langmuir*, 1999, **15**, 6631.